cmgh
CELLULAR AND MOLECULAR GASTROENTEROLOGY AND HEPATOLOGY

ORIGINAL RESEARCH

Deficiency of the Two-Pore Potassium Channel KCNK9 Impairs Intestinal Epithelial Cell Survival and Aggravates Dextran Sodium Sulfate-Induced Colitis

Steffen Pfeuffer,[1,*] Thomas Müntefering,[2,*] Leoni Rolfes,[2] Frederike Anne Straeten,[1] Susann Eichler,[1] Joel Gruchot,[2] Vera Dobelmann,[2] Tim Prozorovski,[2] Boris Görg,[3] Mihael Vucur,[3] Carsten Berndt,[2] Patrick Küry,[2] Tobias Ruck,[2] Stefan Bittner,[4] Dominik Bettenworth,[5] Thomas Budde,[6] Tom Lüdde,[3] and Sven G. Meuth[2]

[1]Institute for Translational Neurology and Neurology Clinic, University of Muenster, Muenster, Germany; [2]Department of Neurology, University Hospital Duesseldorf, Heinrich Heine University Duesseldorf, Duesseldorf, Germany; [3]Department of Gastroenterology, Hepatology and Infectiology, University Hospital Duesseldorf, Heinrich Heine University Duesseldorf, Duesseldorf, Germany; [4]Department of Neurology, University Medical Centre, Johannes Gutenberg University Mainz, Mainz, Germany; [5]Department of Medicine B, Gastroenterology and Hepatology, University Hospital Muenster, Muenster, Germany; and [6]Institute of Physiology 1, University of Muenster, Muenster, Germany

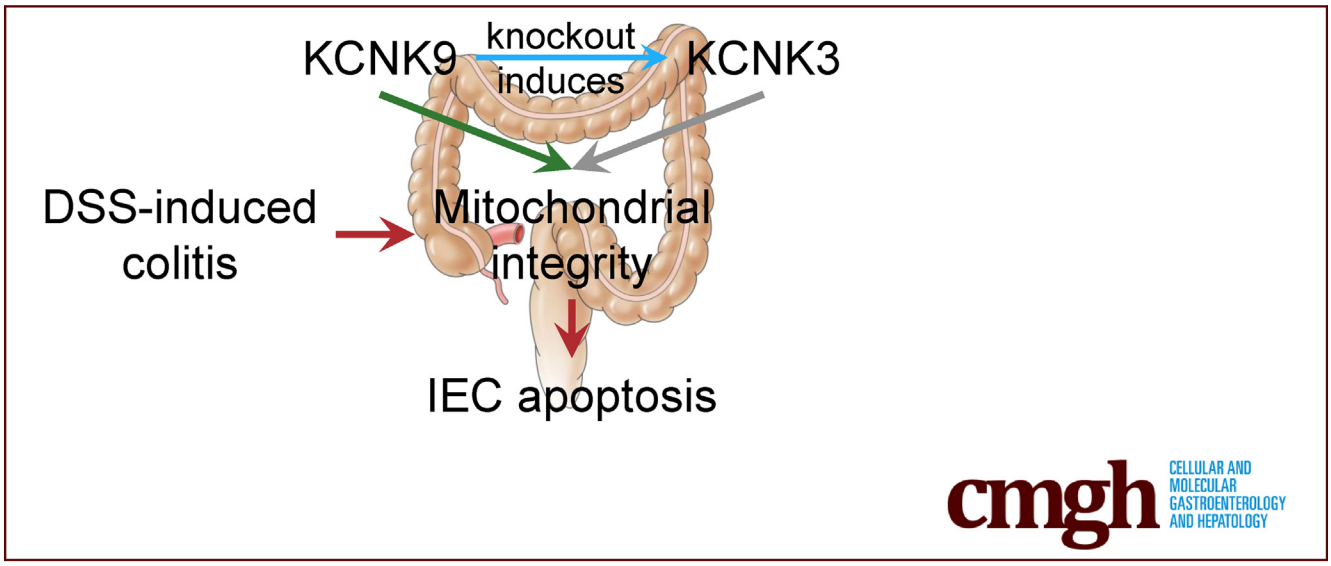

SUMMARY

Deficiency or blockade of the 2-pore potassium channel subfamily K member 9 (KCNK9) aggravates experimentally induced colitis. KCNK9 promotes mitochondrial stability and thus limits caspase-9–dependent apoptosis in intestinal epithelial cells. Lack of KCNK9 cannot be compensated by KCNK3, although the structural similarity is enormous.

BACKGROUND & AIMS: The 2-pore potassium channel subfamily K member 9 (KCNK9) regulates intracellular calcium concentration and thus modulates cell survival and inflammatory signaling pathways. It also was recognized as a risk allele for inflammatory bowel disease. However, it remains unclear whether KCNK9 modulates inflammatory bowel disease via its impact on immune cell function or whether its influence on calcium homeostasis also is relevant in intestinal epithelial cells.

METHODS: *Kcnk9*$^{-/-}$ mice were challenged with 3% dextran sulfate sodium (DSS) to induce experimental acute colitis. Primary cultures of intestinal epithelial cells were generated, and expression of potassium channels as well as cytosolic calcium levels and susceptibility to apoptosis were evaluated. Furthermore, we evaluated whether KCNK9 deficiency was compensated by the closely related 2-pore potassium channel KCNK3 in vivo or in vitro.

RESULTS: Compared with controls, KCNK9 deficiency or its pharmacologic blockade were associated with aggravated DSS-induced colitis compared with wild-type animals. In the absence of KCNK9, intestinal epithelial cells showed increased intracellular calcium levels and were more prone to mitochondrial damage and caspase-9–dependent apoptosis. We found that expression of KCNK3 was increased in *Kcnk9*$^{-/-}$ mice but did not prevent apoptosis after DSS exposure. Conversely, increased levels of KCNK9 in *Kcnk3*$^{-/-}$ mice were associated with an ameliorated course of DSS-induced colitis.

CONCLUSIONS: KCNK9 enhances mitochondrial stability, reduces apoptosis, und thus supports epithelial cell survival after DSS exposure in vivo and in vitro. Conversely, its increased expression in *Kcnk3*$^{-/-}$ resulted in less mitochondrial damage and apoptosis and was associated with beneficial outcomes in DSS-induced colitis. *(Cell Mol Gastroenterol Hepatol 2022; 14:1199–1211; https://doi.org/10.1016/j.jcmgh.2022.08.003)*

Keywords: Two-Pore Potassium Channels; DSS-Induced Colitis; Caspase-9.

The 2-pore potassium channel (K_{2P}) KCNK9 was identified as a major modulator of intracellular calcium (Ca^{2+}) levels and associated signaling pathways.[1] Initially described as a contributor to resting membrane potential in excitable cells such as neurons, evidence for its role in the modulation of signal responses in immune cells has increased in recent years.[2] In experimental autoimmune encephalomyelitis, KCNK9 significantly contributes to immune cell activation and disease severity.[3,4] Furthermore, genetic variants in the *Kcnk9* gene recently were associated with an increased risk for ulcerative colitis, a variant of inflammatory bowel disease (IBD).[5]

Previous work indicated various mechanisms by which KCNK9 and other closely related potassium channels such as KCNK3 modulate the intracellular calcium level, involving G_q-proteins and diacylglycerol as direct negative regulators.[6,7] Thus, a Ca^{2+} level increase ultimately decreases KCNK3- and KCNK9-mediated K^+ conductance. Conversely, compensatory K^+ efflux provides an electrochemical gradient and hence is a prerequisite for Ca^{2+} influx.[8] Notably, previous work indicated that KCNK3 and KCNK9 share most of their structure and properties, and even form heterodimers. Thus, it repeatedly was assumed that the channels can be substituted for one another.[9]

Increased intracellular Ca^{2+} levels are associated with a plethora of signaling responses in intestinal epithelial cells and many of these signals are involved in the pathophysiology of IBD, including the formation and stability of tight junctions and epithelial cell survival.[10] Dysfunction or even loss of epithelial barrier integrity is a hallmark of IBD,[11] and drives chronic disease in addition to prerequisites such as increased activation of immune cells or changes in the intestinal microbiome.[12] IBD is characterized by chronic remittent flares of colitis that can present with abdominal pain, diarrhea, and rectal bleeding.[13]

However, K2P channels do not just share potential interaction points with IBD pathophysiology, but also represent potentially druggable targets. Given its potential link to IBD at a genomic variant level, we decided to investigate the effects of KCNK9 modification in an animal model of IBD and to further elucidate the cellular effects of KCNK9 abrogation on intestinal epithelial calcium homeostasis and cell survival.

Results

KCNK9-Deficient Mice Show Exacerbated Morbidity in Acute Dextran Sulfate Sodium–Induced Colitis

To test whether KCNK9 affects intestinal inflammation, we exposed knockout mice and their respective wild-type controls to 1 course of dextran sulfate sodium (DSS) treatment followed by normal drinking water. *Kcnk9*$^{-/-}$ mice suffered from increased weight loss (Figure 1*A*) and showed more severe clinical symptoms, including diarrhea and rectal bleeding, as depicted by the disease activity index (Figure 1*B*). We examined the intestinal barrier integrity in vivo using fluorescein isothiocyanate–dextran and identified significantly increased barrier disruption in *Kcnk9*$^{-/-}$ mice (Figure 1*E*). Accordingly, both inflammatory colon shortening (Figure 1*D* and *F*) and histology scores (Figure 1*C* and *G*) indicated more severe disease. In line, serum inflammatory cytokine level controls including interleukin (IL)1β, tumor necrosis factor α (TNF-α), and IL6 were found increased in *Kcnk9*$^{-/-}$ mice compared with controls (Figure 1*H*). Notably, we were able to document an increase of caspase-9, but not caspase-8, activation in the intestinal epithelium of *Kcnk9*$^{-/-}$ mice compared with controls (Figure 1*I*)

The Phenotype of KCNK9-Deficient Mice Can Be Reproduced by Pharmacologic Blockade

To validate the detrimental effects caused by genetic knockout in *Kcnk9*$^{-/-}$ mice, we specifically blocked KCNK9 using the recently described substance 1-[1-[6-([1,1′-biphenyl]-4-ylcarbonyl)-5,6,7,8-tetrahydropyrido[4,3-d]pyrimidin-4-yl]-4-piperidinyl]-1-butanone (PK-THPP) in wild-type and knockout animals and again acutely induced colitis with DSS treatment.[14,15] Pharmacologic inhibition of KCNK9 severely affected wild-type animals as indicated by weight loss (Figure 2*A*) and disease activity index (Figure 2*B*), but did not further modify the disease course of knockout animals. Barrier disruption also was more substantial in PK-THPP–treated wild-type animals (Figure 2*E*). Inflammatory colon shortening (Figure 2*D* and *F*) and histology scores (Figure 2*C* and *G*) again were increased. Similarly, serum cytokine levels for IL1β, TNF-α, and IL6 were increased after PK-THPP treatment in wild-type mice (Figure 2*H*). In *Kcnk9*$^{-/-}$ mice, we found no additional effect of PK-THPP treatment compared with injection of the vehicle substance alone. Again, we found increased activation of caspase-9 in the intestinal epithelium of *Kcnk9*$^{-/-}$

***Authors share co-first authorship.**

Abbreviations used in this paper: **A293, 2-(butane-1-sulfonyl-amino)-N-[1-(R)-(6-methoxypyridin-3-yl)-propyl]-benz-amide; DMEM, Dulbecco's modified Eagle medium; DMSO, dimethyl sulfoxide; DSS, dextran sulfate sodium; ER, endoplasmic reticulum; IBD, inflammatory bowel disease; IEC, intestinal epithelial cell; IL, interleukin; JC-1, 5,5',6,6'-tetrachloro-1,1',3,3'-tetraethylbenzimidazolocarbocyanine iodide; K2P, 2-pore potassium (channel); mRNA, messenger RNA; PBS, phosphate-buffered saline; PK-THPP, 1-[1-[6-([1,1′-biphenyl]-4-ylcarbonyl)-5,6,7,8-tetrahydropyrido[4,3-d]pyrimidin-4-yl]-4-piperidinyl]-1-butanone; PCR, polymerase chain reaction; TNF-α, tumor necrosis-factor α.**

Most current article

2352-345X
https://doi.org/10.1016/j.jcmgh.2022.08.003

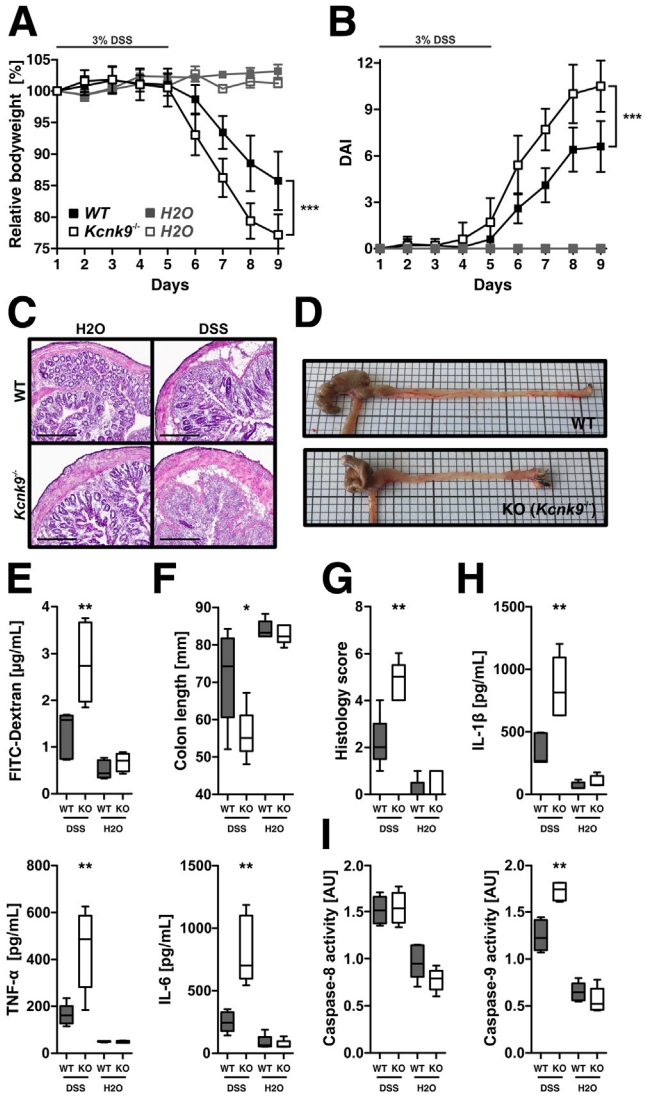

Figure 1. *Kcnk9*$^{-/-}$ mice show increased susceptibility in DSS-induced colitis. (*A* and *B*) Development of body weight (shown as percentage of baseline) and disease activity index (DAI) during acute DSS-induced colitis. DSS was administered from days 1 to 5. (*C*) Generic images of H&E-stained colon sections from DSS-treated animals and controls. *Scale bars*: 300 μm. (*D*) Generic images of explanted colon from DSS-treated wild-type and knockout animals. (*E*) Fluorescein isothiocyanate (FITC)-dextran levels in peripheral blood on day 9. Mice received FITC-dextran 4 hours before sample collection. (*F*) Colon length from anus to ileocecal valve measured from ileocecal valve to anus after explantation. (*G*) Histology score of H&E-stained transverse colon sections. (*H*) Levels of inflammatory cytokines in peripheral blood on day 9. (*I*) Assessment of caspase-8 and caspase-9 activity in colon whole-tissue pieces on day 9. Data are shown as (*A* and *B*) means ± SD or as (*E–I*) box–whisker plots (*boxes* indicate median ± interquartile range, *whiskers* indicate range). (*A* and *B*) n = 10 for DSS-treated and n = 5 for H_2O-treated animals, (*E–I*) n = 5 per group. Statistical significance was tested using 2-way analysis of variance including the (*A* and *B*) Bonferroni post hoc test or the (*E–I*) Mann–Whitney rank-sum test. *P < .05, **P < .01, and ***P < .001. KO, knockout; WT, wild-type.

mice, whereas caspase-8 activation remained equal to controls (Figure 2*I*).

KCNK9 Deficiency Induces Mitochondrial Dysfunction and Increases Apoptosis in Intestinal Epithelial Cells

Next, we generated primary culture of murine colonic intestinal epithelial cells (IECs) from KCNK9-deficient mice and wild-type controls. After 24 hours of cultivation, only a minor fraction of *Kcnk9*$^{-/-}$ IECs underwent apoptosis as indicated by positive caspase-3 staining, and no difference was observed between knockout and wild-type cells (Figure 3*A*). However, *Kcnk9*$^{-/-}$ IECs were prone to cell death after treatment with DSS (TNF-α served as positive control) (Figure 3*B*) and *Kcnk9*$^{-/-}$ IECs showed pronounced activation of caspase-3 (Figure 3*C*). Because it is known that DSS and TNF-α induce apoptosis via different pathways, which are dependent on either initiator caspase-8 or caspase-9,[10,16] we repeated the caspase-3 activation assay after adding DSS and respective inhibitors of the initiator caspases. After adding the fluoromethyl ketone-derived caspase-8 inhibitor, a significant difference still was observed in apoptosis induction in *Kcnk9*$^{-/-}$ IECs after DSS exposure. Conversely, blockade of caspase-9 after adding fluoromethyl ketone-derived caspase-9 inhibitor resulted in a marked reduction in apoptosis and lowering of caspase-3 activation levels in knockout and wild-type IECs (Figure 3*D*).

Because caspase-9 activation is usually the result of organelle damage and the subsequent increase in cytosolic calcium levels, we investigated whether KCNK9 deficiency alters calcium level development over time after DSS exposure of IECs.

We found that *Kcnk9*$^{-/-}$ IECs show a significant increase in late-stage cytosolic calcium levels compared with wild-type controls and that increased levels were maintained (Figure 3*E*). Comparing *Kcnk9*$^{-/-}$ IECs kept in standard medium with those kept in calcium-free medium, we observed differences in the early phase (minutes 5–10) after stimulation with DSS, but no differences in late-stage calcium levels (minutes 10–15) were seen (Figure 3*F*). We concluded that the early increase in cytosolic Ca^{2+} levels results from the influx of extracellular Ca^{2+}, whereas further increases are caused by Ca^{2+} release from internal storage. Notably, differences in caspase-3 activation remained significant between knockout and wild-type cells even in Ca^{2+}-free medium, suggesting that KCNK9 might predominantly affect the release of Ca^{2+} from internal stores (Figure 3*G*).

Different intracellular calcium storing organelles exist, with the endoplasmic reticulum (ER) often being deemed the most important.[17] ER damage and subsequent Ca^{2+} release are an established consequence of ER stress, which can be induced by various mechanisms such as accumulation of unfolded or misfolded proteins. Furthermore, ER stress is well described in IBD and its animal models including DSS-induced colitis.[18] Thus, we investigated whether differences in cytosolic calcium levels originate from increased release of ER-stored calcium. We depleted ER calcium in knockout and wild-type IECs by thapsigargin-

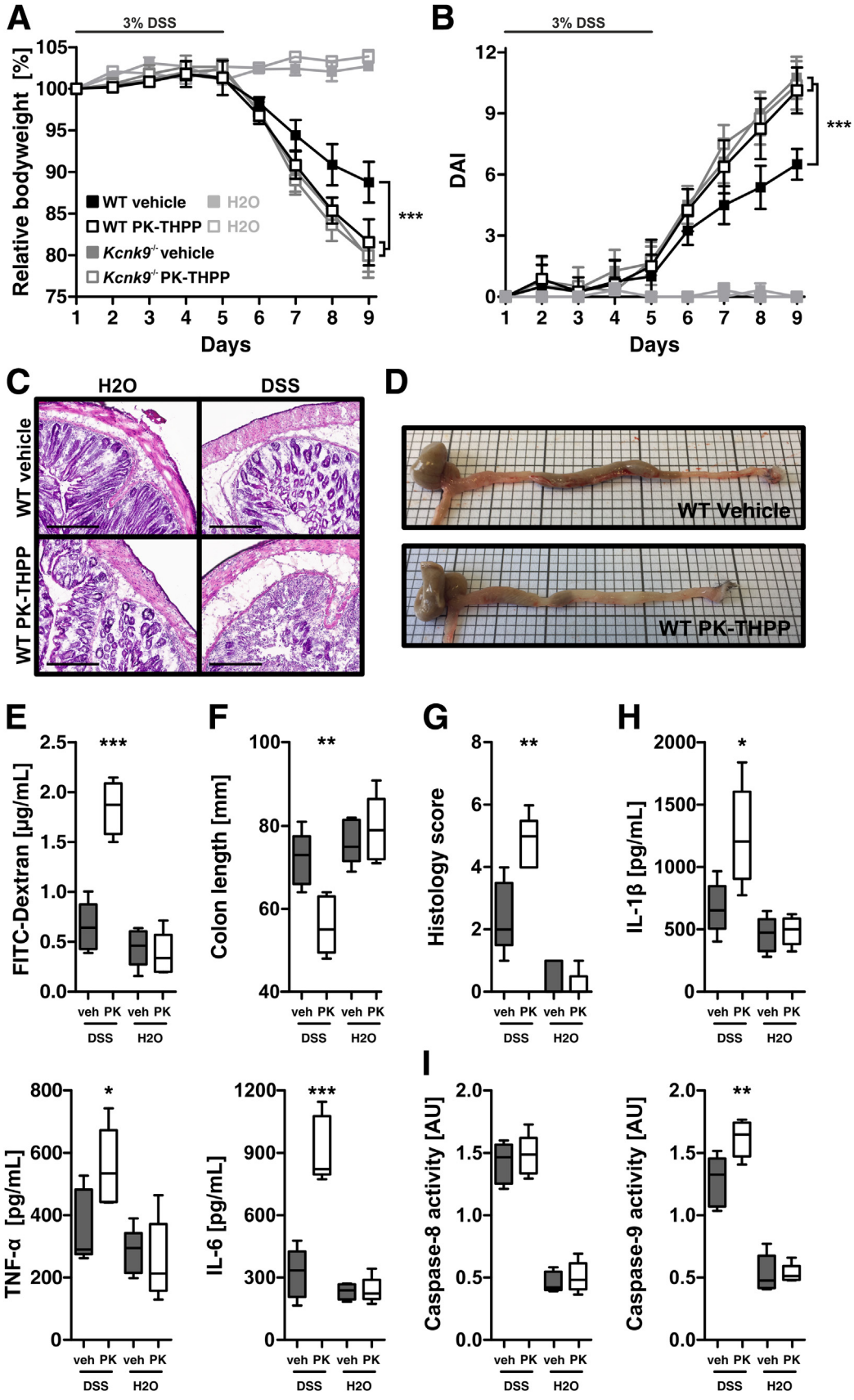
A
3% DSS
Relative bodyweight [%]
105
100
95
90
85
80
75
1 2 3 4 5 6 7 8 9
Days
WT vehicle
H2O
WT PK-THPP
H2O
Kcnk9-/- vehicle
Kcnk9-/- PK-THPP
***
B
3% DSS
DAI
12
9
6
3
0
1 2 3 4 5 6 7 8 9
Days
***
C
H2O
DSS
WT vehicle
WT PK-THPP
D
WT Vehicle
WT PK-THPP
E
FITC-Dextran [µg/mL]
2.5
2.0
1.5
1.0
0.5
0.0
***
veh PK veh PK
DSS H2O
F
Colon length [mm]
100
80
60
40
**
veh PK veh PK
DSS H2O
G
Histology score
8
6
4
2
0
**
veh PK veh PK
DSS H2O
H
IL-1β [pg/mL]
2000
1500
1000
500
0
*
veh PK veh PK
DSS H2O
TNF-α [pg/mL]
800
600
400
200
0
*
veh PK veh PK
DSS H2O
IL-6 [pg/mL]
1200
900
600
300
0
***
veh PK veh PK
DSS H2O
I
Caspase-8 activity [AU]
2.0
1.5
1.0
0.5
0.0
veh PK veh PK
DSS H2O
Caspase-9 activity [AU]
2.0
1.5
1.0
0.5
0.0
**
veh PK veh PK
DSS H2O

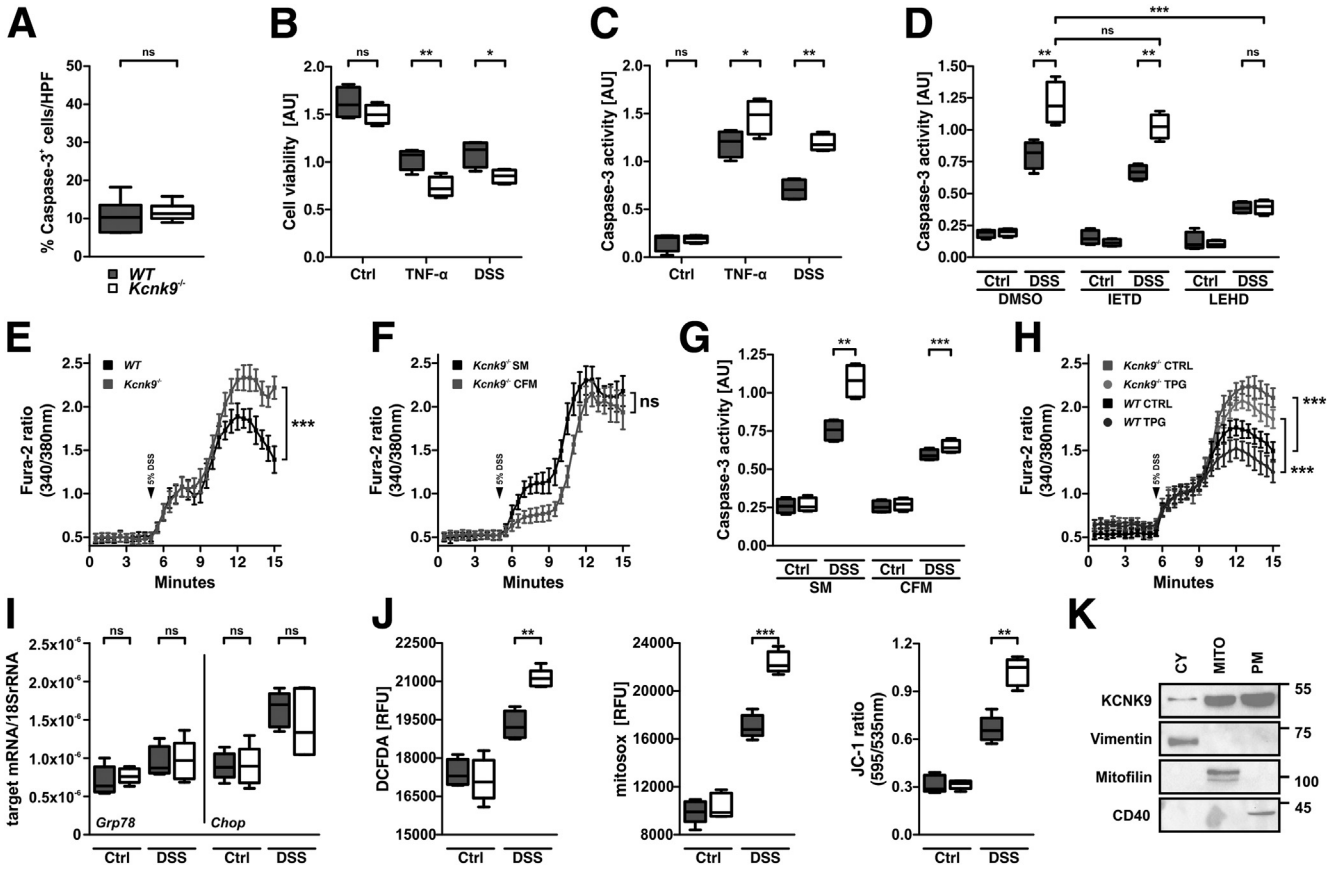

Figure 3. KCNK9 modulates cellular calcium responses and cell survival in IECs. (*A*) Immunofluorescence staining of isolated IECs showing the fraction of apoptotic cells by determination of caspase-3 activation. (n = 5 per group; legend also applies to *B–D*, *G*, *I–K*). (*B*) Evaluation of cell viability after TNF-α and DSS exposure using the Tetrazolium chloride (MTS) assay (n = 5 per group). (*C*) Analysis of caspase-3 activation (n = 5 per group). Caspase-3 activation after DSS treatment with the addition of either DMSO (vehicle), fluoromethyl ketone-derived caspase-8 inhibitor (IETD), fluoromethyl ketone-derived caspase-9 inhibitor (LEHD) in IECs (n = 5 per group). (*E* and *F*) Fura-2–based assay for detecting cytosolic calcium levels in IECs after DSS exposure. *Arrows* indicate addition of 5% DSS solution (n = 8 per group). (*G*) Caspase-3 activation in SM and CFM after DSS exposure (n = 5 per group). (*H*) Fura-2–based assay for detecting cytosolic calcium levels in IECs after DSS exposure after ER calcium depletion using thapsigargin (n = 8 per group). (*I*) Assessment of ER stress marker gene *Grp78* and *Chop* expression in IECs after DSS treatment vs controls (n = 5 per group). (*J*) Quantification of mitochondrial membrane integrity (JC-1), superoxide generation (MitoSOX), and formation of hydroxyl radical via the Fenton reaction (2′,7′-dichlorofluorescin diacetate [DCFDA]) after DSS stimulation (n = 5 per group). (*K*) Western blot of KCNK9 and respective cell fraction markers (numbers on the right indicate mass in kilodaltons). Statistical significance was tested using the (*A–C*, *G*, *I*, and *J*) Mann–Whitney *U* test, (*D*) Kruskal–Wallis test including the Dunn post hoc test, or (*E*, *F*, and *H*) 2-way analysis of variance including the Bonferroni post hoc test. $^{*}P < .05$, $^{**}P < .01$, $^{***}P < .001$, $p > .05$ was not significant. AU, adsorption unit; CFM, calcium-free medium; Ctrl, control; CY, cytosolic fraction; HPF, high-power field; MITO, mitochondrial fraction; PM, plasma membrane fraction; rRNA, ribosomal RNA; SM, standard medium; RFU, relative fluorescent unit; TPG, thapsigargin; WT, wild-type.

Figure 2. (***See previous page***). **Pharmacologic blockade of KCNK9 aggravates DSS-induced colitis in wild-type mice.** (*A* and *B*) Development of body weight (shown as percentage of baseline) and disease activity index (DAI) during acute DSS-induced colitis. DSS was administered from days 1 to 5. (*C*) Generic images of H&E-stained colon sections from DSS-treated animals and controls. *Scale bars*: 300 μm. (*D*) Generic images of explanted colon from DSS-treated wild-type and knockout animals. (*E*) Fluorescein isothiocyanate (FITC)-dextran levels in peripheral blood on day 9. Mice received FITC-dextran 4 hours before sample collection. (*F*) Colon length from the anus to the ileocecal valve measured from the ileocecal valve to the anus after explantation. (*G*) Histology score of the H&E-stained transverse colon sections. (*H*) Levels of inflammatory cytokines in peripheral blood on day 9. (*I*) Assessment of caspase-8 and caspase-9 activity in colon whole-tissue pieces on day 9. Data are shown as the (*A* and *B*) means ± SD or as (*E–I*) box-whisker plots (*boxes* indicate median ± interquartile range, *whiskers* indicate range). (*A* and *B*) n = 10 for DSS-treated and n = 5 for H_2O-treated animals, (*E–I*) n = 5 per group. Statistical significance was tested using 2-way analysis of variance including the (*A* and *B*) Bonferroni post hoc test or the (*E–I*) Mann–Whitney rank sum test. $^{*}P < .05$, $^{**}P < .01$, and $^{***}P < .001$. veh, vehicle; WT, wild-type.

induced blockade of the ER calcium adenosine triphosphatase (SERCA) and measured cytosolic calcium levels after DSS exposure. Thapsigargin treatment resulted in comparable lowering of peak cytosolic calcium levels in both knockout and wild-type cells (reduction of the peak Fura-2 ratio in knockout cells by 0.167 adsorption units (7.46%) vs 0.245 adsorption units (13.8%) (Figure 3*H*). However, differences between knockout and wild-type animals persisted and therefore we concluded that increased Ca^{2+} levels in *Kcnk9*$^{-/-}$ originate from organelles other than the ER. Furthermore, we observed no differences in expression of ER stress marker genes after DSS treatment (Figure 3*F*)

Mitochondria also contain substantial calcium stores and the presence of KCNK9 on mitochondria has been reported previously.[19] We explored whether these organelles might be less resistant to DSS exposure in the absence of KCNK9 and used fluorescent dyes to visualize mitochondrial response toward DSS. KCNK9 deficiency boosted both mitochondrial membrane depolarization (measured via 5,5′,6,6′-tetrachloro-1,1′,3,3′-tetraethylbenzimidazolocarbocyanine iodide [JC-1] assay) and mitochondrial superoxide production (measured via MitoSOX oxidation). Consequently, hydrogen peroxide is increased as measured by an increased Fenton reaction via 2′,7′-dichlorofluorescin diacetate oxidation (all Figure 3*J*). Because we hypothesized that KCNK9 might regulate mitochondrial integrity, we performed Western blot of isolated cell fractions and found that KCNK9, in addition its presence on the plasma membrane, also was present in the mitochondrial fraction (Figure 3*K*).

IECs React to KCNK9 Deficiency via Up-Regulation of KCNK3

As described earlier, KCNK9 shares most of its properties with its closest relative KCNK3, aside from the formation of heterodimers.[6,20] To test the relevance of this resemblance in IECs, we screened *Kcnk9*$^{-/-}$ and wild-type control cells for differential expression of the known 2-pore potassium channels. KCNK9 deficiency resulted in a strong increase of *Kcnk3* gene expression, whereas expression levels of other K_{2P} channels remained largely unaltered (Figure 4*A*). Expression of KCNK3 and KCNK9 were visualized at the protein level via immunofluorescence staining (Figure 4*B*).

To further elucidate the role of a potential interplay between KCNK3 and KCNK9, we used the experimental inhibitor substance 2-(butane-1-sulfonyl-amino)-N-[1-(R)-(6-methoxypyridin-3-yl)-propyl]-benz-amide (A293), which preferably inhibits KCNK3 (and to a very minimal extent KCNK9) channel function.[4] Its administration led to no relevant decrease of apoptosis in wild-type IECs after DSS exposure. However, its effect was potentiated in *Kcnk9*$^{-/-}$ IECs, corroborating the high *Kcnk3* gene expression (Figure 4*C*). Remarkably, we observed a decrease in apoptosis rate even below values found in A293-treated wild-type IECs, and we presume that in the absence of KCNK3 and KCNK9 channel function, Ca^{2+} influx is largely suppressed in general. In line with this, we detected a decrease of late-stage cytosolic calcium levels in DSS-exposed *Kcnk9*$^{-/-}$ IECs after incubation with A293 (Figure 4*D*).

We then sought to establish whether KCNK3 exerts a specific role in modulation of Ca^{2+} influx or whether the observed phenomena are owing to transcriptional effects. We silenced channel functions by pharmacologic inhibition in wild-type IECs. First, we specifically blocked KCNK9 by adding PK-THPP before DSS exposure, and 5 minutes after DSS administration we added A293. We found that PK-THPP treatment closely resembled the phenotype observed in *Kcnk9*$^{-/-}$ IECs, whereas A293 treatment had no demonstratable effect on late-stage Ca^{2+} influx alone but led to a potent decrease of cytosolic Ca^{2+} levels when administered subsequently to PK-THPP (Figure 4*E*).

Subsequently, we decided to verify our results in a genetic knockout of KCNK3. Examining the DSS-induced increase of cytosolic calcium levels confirmed our previous finding and showed a significant decrease of late-stage calcium influx in *Kcnk3*$^{-/-}$ IECs (Figure 4*F*). In those cells, we found a reciprocal increase in *Kcnk9* messenger RNA (mRNA) expression, whereas the absence of *Kcnk3* mRNA was shown by real-time polymerase chain reaction (PCR) (Figure 4*G*). We evaluated mitochondrial function via the previously performed assays and detected reduced mitochondrial superoxide production as well as greater persistence of mitochondrial membrane potential (both Figure 4*H*). However, these effects appear to be caused by increased KCNK9 channel expression because elimination of this aspect by pharmacologic blockade with A293 again yielded no respective phenotype in wild-type IECs.

KCNK3-Deficient Mice Are Protected From Acute DSS-Induced Colitis

Lastly, we subjected *Kcnk3*$^{-/-}$ mice and their respective wild-type controls to DSS-induced colitis. We found that KCNK3 deficiency reduced weight loss and disease activity index compared with wild-type controls (Figure 5*A* and *B*). Barrier disruption was reduced, although effects were not statistically significant here (Figure 5*E*). However, colonic shortening (Figure 5*D* and *F*) as well as histologic damage were markedly less pronounced (Figure 5*C* and *G*). We also observed lower levels of inflammatory cytokines in peripheral blood samples obtained from our knockout mice compared with control animals (Figure 5*I*). Lastly, we performed expression analysis of *Kcnk9* mRNA from colon samples and confirmed increased expression in Kcnk3$^{-/-}$, thereby confirming our previous results from IEC studies. Notably, here we found increased expression of KCNK9 in DSS-treated wild-type animals compared with water controls ($P = .0317$) (Figure 5*H*). Similar to DSS-induced colitis experiments in *Kcnk9*$^{-/-}$ mice, we performed activation assays regarding caspase-8 and caspase-9 and found unaltered levels of caspase-8 activation whereas caspase-9 activation was reduced in *Kcnk3*$^{-/-}$ mice compared with controls (Figure 5*J*).

Discussion

Within the presented work, we aimed to establish a deeper understanding of the potential role of KCNK9 in epithelial cell survival and its in vivo impact on DSS-induced colitis. We found that, as well as the genetic knockout, pharmacologic blockade of KCNK9 aggravated DSS-induced colitis including more pronounced weight loss, more

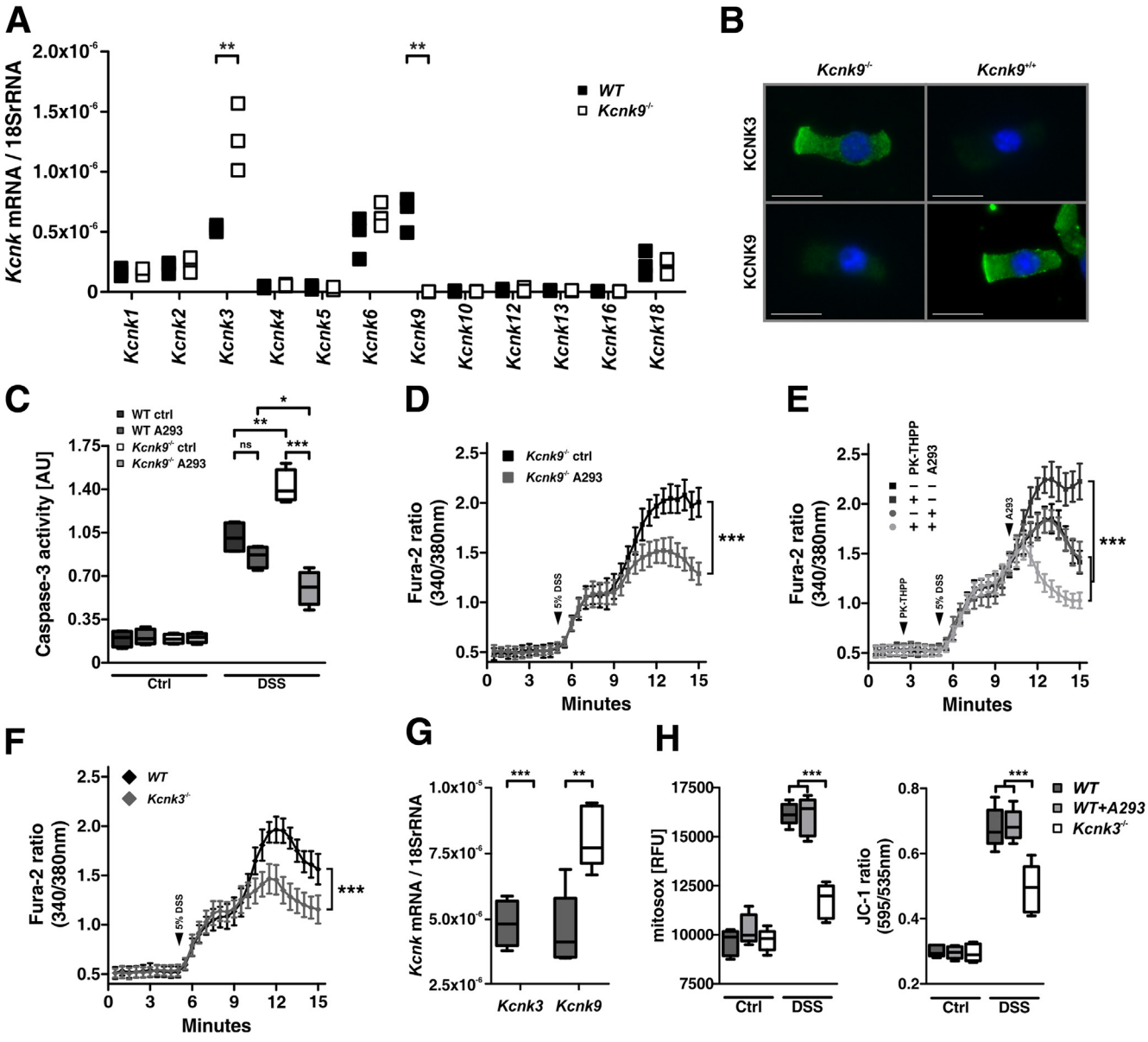

Figure 4. *Kcnk9*$^{-/-}$ IECs show up-regulation of *Kcnk3* mRNA and blockade of KCNK3 normalizes calcium responses. (*A*) Analysis for gene expression of different K_{2P} channels in untreated *Kcnk9*$^{-/-}$ and wild-type IECs using quantitative real-time PCR (n = 3 per group). (*B*) Immunofluorescence analysis for validating channel expression on the protein level in IECs. *Columns* indicate genotype, *rows* indicate performed staining. Nuclear staining was performed with 4',6-diamidino-2-phenylindole. *Scale bars*: 10 μm. (*C*) Caspase-3 activation after DSS stimulation and addition of KCNK3 and caspase-9 inhibitor A293 (n = 5 per group). (*D*) Calcium assay after A293 addition (n = 8 per group). (*E*) Calcium assay after PK-THPP and/or A293 addition and DSS stimulation (n = 8 per group). (*F*) Calcium assay in *Kcnk3*$^{-/-}$ IECs (n = 8 per group). (*G*) mRNA expression of *Kcnk3* and *Kcnk9* in *Kcnk3*$^{-/-}$ IECs (n = 5 per group). (*H*) Evaluation of mitochondrial superoxide generation (MitoSOX) and mitochondrial membrane integrity (JC-1) after DSS stimulation (n = 5 per group). Statistical significance was tested using the (*A* and *G*) Mann–Whitney *U* test, (*C* and *H*) Kruskal–Wallis test including Dunn post hoc test, or (*D*–*F*) 2-way analysis of variance including the Bonferroni post hoc test. *$P < .05$, **$P < .01$, ***$P < .001$; $p > .05$ was not significant. AU, adsorption unit; Ctrl, control; RFU, relative fluorescent unit; rRNA, ribosomal RNA; WT, wild-type.

severe clinical symptoms, and impairment of intestinal epithelial barrier function with subsequent release of inflammatory cytokines. After establishment of primary colonic IEC cultures from knockout and wild-type animals, we found increased susceptibility of *Kcnk9*$^{-/-}$ IECs to apoptosis after DSS exposure and, similar to in vivo data, we showed a major role for caspase-9 activation and thus the intrinsic apoptosis cascade. Intracellular calcium levels increased more strongly after DSS treatment in the absence or blockade of KCNK9 and we were able to identify mitochondrial damage as the underlying cause for the excessive increase of cytosolic Ca^{2+} levels, whereas we found no specific predisposition to ER stress. Although closely related to KCNK9 regarding structure and function, and up-

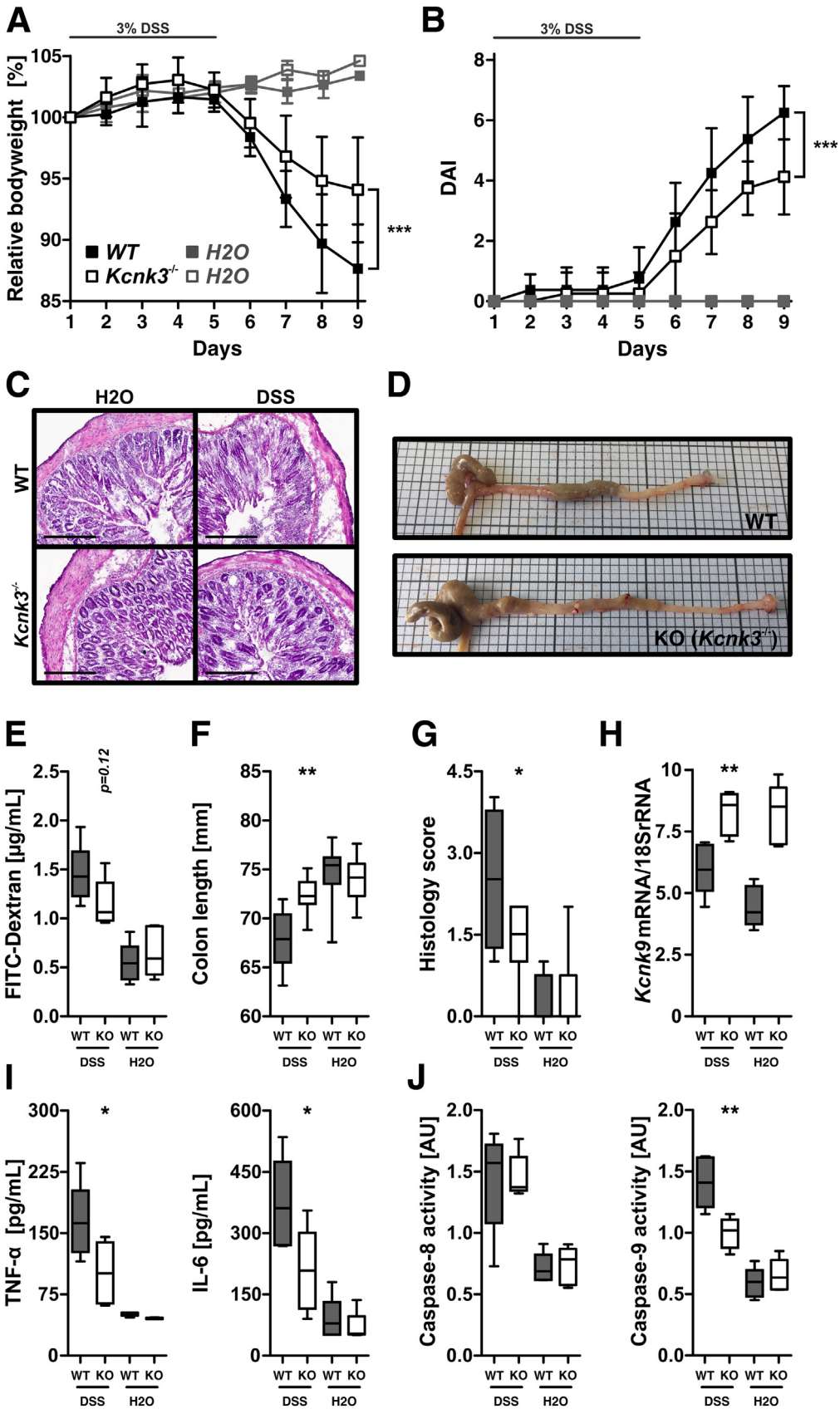

Figure 5. *Kcnk3*$^{-/-}$ mice show ameliorated courses compared with controls in DSS-induced colitis. (*A* and *B*) Development of body weight (shown as percentage of baseline) and disease activity index (DAI) during acute DSS-induced colitis. DSS was administered from days 1 to 5. (*C*) Generic images of H&E-stained colon sections from DSS-treated animals and controls. *Scale bars*: 300 μm. (*D*) Generic images of explanted colon from DSS-treated wild-type and knockout animals. (*E*) Fluorescein isothiocyanate (FITC)-dextran levels in peripheral blood on day 9. Mice received FITC-dextran 4 hours before sample collection. (*F*) Colon length from the anus to the ileocecal valve measured from the ileocecal valve to the anus after explantation. (*G*) Histology score of H&E-stained transverse colon sections. (*H*) Quantitative assessment of *Kcnk9* mRNA expression in colon whole-tissue pieces on day 9. (*I*) Levels of inflammatory cytokines in peripheral blood on day 9. (*J*) Assessment of caspase-8 and caspase-9 activity in colon whole-tissue pieces on day 9. Data are shown as (*A* and *B*) means ± SD or as (*E*–*J*) box-whisker plots (*boxes* indicate median ± interquartile range, *whiskers* indicate range). (*A* and *B*) n = 10 for DSS-treated and n = 5 for H_2O-treated animals, and (*E*–*J*) n = 5 per group. Significance was calculated using 2-way analysis of variance including the (*A* and *B*) Bonferroni post hoc test or the (*E*–*J*) Mann–Whitney *U* test. **P* < .05, ***P* < .01, ****P* < .001. FITC, fluorescein isothiocyanate; KO, knockout; rRNA, ribosomal RNA; WT, wild-type.

regulated in *Kcnk9*$^{-/-}$ IECs, KCNK3 could not compensate for the loss of KCNK9 function. Conversely, the beneficial effects of KCNK3 deficiency regarding DSS-induced Ca^{2+} influx, mitochondrial damage, and apoptosis were accompanied by stronger expression of KCNK9. Similar observations also were made in *Kcnk3*$^{-/-}$ mice that underwent DSS-induced colitis.

It generally is accepted that DSS mediates its effects on the intestinal epithelium through a number of mechanisms, including the development of ER stress, Ca^{2+}-dependent breakdown of tight junction proteins, and, ultimately, apoptosis, and DSS therefore at least partially resembles the pathophysiology of ulcerative colitis.[10,21] Analysis of cytosolic Ca^{2+} responses toward DSS exposure showed a 2-step increase of Ca^{2+}. The first step was significantly reduced in Ca^{2+}-free medium and was preserved in thapsigargin-treated IECs and thus most likely represents influx of Ca^{2+} from the extracellular space. Although KCNK9 was described to modulate this Ca^{2+} via provision of a compensatory potassium efflux in various cell types,[3,19,22–24] we found no difference in *Kcnk9*$^{-/-}$ IECs compared with controls. However, the second step of cytosolic Ca^{2+} increase, which was reduced (but not absent) after thapsigargin treatment and resistant to Ca^{2+}-free medium and thus represents release of Ca^{2+} from internal storage, was strongly increased in KCNK9 deficiency. Although the majority of Ca^{2+} released within calcium-induced calcium release comes from the ER,[25,26] we found no restitution of *Kcnk9*$^{-/-}$ IECs by thapsigargin. Furthermore, ER stress was rendered as an unlikely cause of the observed phenotype because induction of ER stress upon thapsigargin treatment did not copy the differences between wild-type and KCKN9-deficient mice in terms of cytosolic calcium levels and we observed no increases in ER stress-response genes in knockout IECs compared with wild-type controls.

However, we were able to show rapid impairment of mitochondrial integrity after DSS exposure in *Kcnk9*$^{-/-}$ IECs, resulting in permeabilization of the outer membrane and loss of the mitochondrial membrane potential depicted in our JC-1 staining.

Mitochondrial stress is induced by DSS via different pathways. First, reactive oxygen species are known to disturb the redox equilibrium of mitochondria in DSS-induced colitis.[27] Second, regeneration of mitochondria by fission and fusion is impaired after DSS exposure.[28] Finally, ER stress itself impairs mitochondrial function by interference with Ca^{2+} transport between ER and mitochondria.[29]

Interestingly, our data also showed that KCNK9 was not restricted to the plasma membrane but also was found on the mitochondrial membrane. Several potassium channels localized on mitochondria have been shown to ameliorate mitochondrial damage and subsequent cell death by limitation of Ca^{2+} currents.[30,31] Interestingly, DSS itself induces the mitogen-activated protein kinase/extracellular signal-activated kinase (MAPK/ERK) signaling cascade und thereby enhances mitochondrial Ca^{2+} release via increased expression of transport proteins calcium release-activated calcium channel protein 1 (ORAI1) and stromal interaction molecule (STIM).[32] Notably, DSS also induced increased expression of KCNK9 in wild-type IECs, thus presenting a potential mechanism for fine-tuning mitochondrial Ca^{2+} efflux.

It currently only can be speculated how KCNK9 is able to limit mitochondrial toxicity, but recent data have indicated that synthesis of diacyl glycerol after $Ca2^{+}$ release and activation of Gq-proteins inhibits KCNK9 function and thus reduces the rectifying potassium current required for further release of Ca^{2+}.[6] Furthermore, KCNK9 is acid-sensitive and the channel closes secondary to reduced pH, which regularly occurs during mitochondrial stress, further reducing conductance.[2] In line, previous work has shown impairment of mitochondrial function in the absence of KCNK9 in keratinocytes.[33]

Mitochondrial permeabilization results in the release of cytochrome c as well as further pro-apoptotic factors and thus is capable of activating caspase-9 and inducing apoptosis, as previously observed.[34] Notably, TNF-α also is capable of inducing mitochondrial disintegration[35] and this explains the increased susceptibility of *Kcnk9*$^{-/-}$ IECs to TNF-α exposure in our experiments. We assume that these mechanisms are pivotal to the loss of intestinal barrier function and more severe courses of DSS-induced colitis.

Nonetheless, we were largely surprised to see that KCNK3 was incapable of compensating for KCNK9 deficiency despite its well-known mechanism of compensatory regulation. Protein sequences of both channels are largely similar and previous work has indicated similar properties throughout.[2,36] Even more, channels can form functional heterodimers as well.[9] Because we observed a reduction of cytosolic Ca^{2+} increase, mitochondrial damage in *Kcnk3*$^{-/-}$ IECs, as well as ameliorated DSS-induced colitis in Kcnk3$^{-/-}$ mice, one could assume that both channels mediate opposite functions. However, pharmacologic blockade using the KCNK3 inhibitor A293 restored phenotypes of Kcnk9$^{-/-}$ IECs but did not alleviate findings in wild-type cells. This contrasts blockade of KCNK9 by its specific inhibitor, which copies the disease phenotype of *Kcnk9*$^{-/-}$ IECs. What indeed was found in vitro as well as in vivo was that KCNK3 deficiency increases *Kcnk9* expression, which was not entirely unexpected given the assumption of a common, yet still unknown, promotor.[6,36] We thus assume that increased expression of KCNK9 as observed in vitro and in vivo within DSS-induced colitis modulates the phenotype rather than absence of KCNK3.

It is not clear how A293 selectively restores the phenotype of the further reduction of Ca^{2+} influx by A293 in both *Kcnk9*$^{-/-}$ IECs and PK-THPP–exposed wild-type IECs. However, it is likely that a lack of KCNK3/9 potassium conductance largely alters cellular homeostasis beyond mitochondrial function. Unfortunately, it is not possible to further investigate this given the absence of KCNK3$^{-/-}$// KCNK9$^{-/-}$ double-knockout mice.

In conclusion, we have shown that KCNK9 positively modulates intestinal epithelial cell survival in the context of intestinal inflammation in vitro and in vivo. Future studies should target strategies to induce overexpression or enhance channel function to boost IEC survival in the context of inflammatory conditions.

Methods

Animals

The development of the *Kcnk3*$^{-/-}$ and *Kcnk9*$^{-/-}$ mouse models has been described previously.[4] Animals were raised on a C57Bl/6J background and crossed-back at least 10 times before use. For experiments, we used knockout animals and their respective wild-type littermates (abbreviated as wild-type throughout text). Animals were kept in specific pathogen-free conditions and fed a standard rodent diet. Local authorities approved all animal experiments (84-02.04.2012.A441; North Rhine-Westphalian Ministry for Environment, Health and Consumer Protection, Department for Animal Protection).

Experimental Model of Colitis and Barrier Permeability Assay

Mice (age, 8–10 weeks) with their respective genetic background were exposed to a 3% aqueous solution of DSS (36–50 kilodaltons; MP Biomedicals, Eschwege, Germany) ad libitum via drinking water for 5 consecutive days. Given the reduced breeding efficiency of K2P-deficient mice (a well-known phenomenon), strict local regulations for animal breeding and the need for female animals elsewhere (including strain maintenance), and the known variation of disease severity during the ovarian cycle,[37] male animals were used here.

Furthermore, drinking solution was prepared fresh every 24 hours and consumption per cage was documented for estimation of DSS uptake per mouse (no significant differences were noted here). On days 6–9, mice received normal drinking water. One experimental group received PK-THPP, a potent antagonist of KCNK9,[14,15] which was administered intraperitoneally once daily throughout the experiment (10 μg/g body weight in 200 μL 1% dimethyl sulfoxide [DMSO]/40% polyethylene glycol 400/phosphate-buffered saline [PBS]) Sigma Aldrich, St. Louis, MO). Control animals received 200 μL 1% DMSO/40% polyethylene glycol 400/PBS intraperitoneally. Animals were assessed daily for body weight, stool consistency, and rectal bleeding. Occult rectal bleeding was determined using the Hemoccult test (Beckman Coulter, Brea, CA). On day 9, blood and colon samples were taken for further analysis. The disease activity index score during the experiment and the histology scores were calculated as previously described.[38] Serum cytokine levels were assessed using enzyme-linked immunosorbent assays for the respective cytokines (Thermo Fisher Scientific, Waltham, MA) according to the manufacturer's protocol. For barrier permeability assay, mice received 0.5 mg/g fluorescein isothiocyanate–dextran (average molecular weight, 3–5 kilodaltons; Sigma Aldrich) via oral gavage. After 4 hours, blood samples were taken and sera were measured at 490 nm.

Isolation of Primary IECs

For isolation of primary IECs, colons were harvested from 8-week-old naïve male mice. After flushing with ice-cold PBS, the colon was opened longitudinally and cut into small pieces. Tissue pieces were transferred to a 50-mL tube containing 30 mL 1.5 mmol/L EDTA in Hank's balanced salt solution (Sigma Aldrich) and placed horizontally on an orbital shaker for 10 minutes at 37°C. The supernatant was discarded and 15 mL fresh 1.5 mmol/L EDTA in Hank's balanced salt solution was added. Tubes then were vortexed for 1 minute, and the supernatant was collected. This procedure was repeated twice. Supernatants then were combined and centrifuged for 10 minutes at 300 $\times$ g. Cells were washed and resuspended in Dulbecco's modified Eagle medium (DMEM) containing 20% fetal calf serum (Thermo Fisher), 1% penicillin/streptomycin cocktail (Thermo Fisher), and 100 ng/mL recombinant murine epidermal growth factor (R&D Systems, Minneapolis, MN). Culture plates were coated with fibronectin/collagen IV (both Thermo Fisher) for 2 hours in advance at 37°C. Cells were counted using a CASY TT cell counter (Omni Life Sciences, Bremen, Germany). Cells were cultured for 24 hours before the respective experiments.

Cell Viability and Caspase Activation Assay

For cell viability analysis, cells were seeded on a 96-well plate (0.75 $\times$ 10^5 cells/well) as described earlier. Eight hours after stimulation with either Tnf-α (50 μg/mL) or DSS (3%), media were replaced with 100 μL PBS containing 20% v/v Tetrazolium chloride (MTS) reagent (Abcam, Cambridge, UK), and cells were kept for 45 minutes. Optical density was assessed at 490 nm using a microplate reader (Tecan, Mennedorf, Switzerland).

To determine caspase-3 activation, a commercial assay (Abcam) was used according to the manufacturer's recommendations. Plates were read at 405 nm. The caspase inhibitors LEHD (tetrapeptide inhibitor for caspase-8; 20μM; R&D Systems), IETD (tetrapeptide inhibitor for caspase-9; 20μM; R&D Systems) or vehicle substance (1% DMSO) were added 30 min prior to stimulation. For determination of caspase-8 and caspase-9 activation in the intestinal epithelium after DSS-induced colitis, protein lysates were prepared from colon whole-tissue pieces using denaturing lysis buffer (described by Kwon et al[39]) and protein concentration was evaluated using the DC protein assay kit (Thermo Fisher). Samples were adjusted to a total protein concentration of 200 μg/mL and caspase activation was determined using colorimetric assays for caspase-8 and caspase-9 activation, according to the manufacturer's protocol (Abcam).

Mitochondria Isolation and Western Blot

Mitochondria and cytosolic cell fractions were isolated from primary IECs (5 $\times$ 10^6 cells) using a commercial mitochondria isolation kit (Thermo Fisher Scientific), according to the manufacturer's recommendations. Plasma membranes were isolated following the previously published protocol by Kwon et al.[39] Western blot was performed as described before.[22] Antibodies were used as follows: anti-KNCK9 (P5247, 1:1000; Sigma Aldrich),

antivimentin (D21H3, 1:2000; CST), antimitofilin (ab205718, 1:2000; Abcam), and anti-CD40 (ab13545, 1:1500; Abcam). A horseradish-peroxidase–conjugated secondary antibody was used for chemiluminescent labeling (anti-rabbit-IgG, A3682, 1:10,000; Sigma Aldrich).

RNA Isolation and Quantitative Real-Time PCR

Cultured intestinal epithelial cells were harvested and RNA was isolated using the Quick-RNA Miniprep kit (Zymo Research, Freiburg, Germany) according to the manufacturer's instructions, including the optional DNA digestion protocol. Synthesis of complementary DNA was performed using the Maxima H Minus First Strand Synthesis Kit (Fermentas, Waltham, MA) according to the protocol recommended by the manufacturer. Real-time PCR was performed using premanufactured probes (Applied Biosystems, Waltham, MA) according to Table 1. Assays were run on a StepOne Plus Thermocycler (Applied Biosystems).

Table 1. List of TaqMan Probes Used in the Text Including Unique IDs From the Manufacturer's Database (Thermo Fisher)

Gene	TaqMan assay ID
Kcnk1	Mm00434624_m1
Kcnk2	Mm01323942_m1
Kcnk3	Mm04213388_s1
Kcnk4	Mm00434626_m1
Kcnk5	Mm00498900_m1
Kcnk6	Mm01176312_g1
Kcnk9	Mm02014295_s1
Kcnk10	Mm00504118_m1
Kcnk12	Mm02344857_m1
Kcnk13	Mm00524725_m1
Kcnk16	Mm01279322_m1
Kcnk18	Mm01702237_m1
Grp78	Mm00517691_m1
Chop	Mm01135937_g1
18S rRNA	Hs99999901_s1

NOTE. PCR was performed using the StepOne Plus system (Thermo Fisher) with predesigned TaqMan probes (Thermo Fisher). 18S ribosomal RNA probes were used as reference. The prespecified PCR protocol was used as recommended by the manufacturer.

Detection of Intracellular Calcium Concentration and Mitochondrial Function

After isolation, 0.75×10^5 cells per well were cultured for 24 hours in the presence of epidermal growth factor in a 96-well plate coated with fibronectin/collagen IV for 24 hours as described earlier. Before the experiment, the medium was removed and replaced with 100 μL DMEM without phenol red containing 5 μmol/L of the Ca^{2+}-sensitive fluorescent dye Fura-2–AM (Abcam). After 30 minutes, the medium was changed to DMEM without phenol red. After 15 minutes, plates were placed in the microplate reader (excitation wavelengths, 340 nm and 380 nm) and emission was determined at 510 nm every 30 seconds. After 5 minutes of measurement, 50 μL DSS dissolved in PBS was added to a final concentration of 5% DSS via the plate reader's dispenser pumps. Further substances were added as described in the respective experiments (thapsigargin: 1 μmol/L final concentration, treatment 4 hours before the experiment; A293: 10 μmol/L final concentration, kindly provided by Sanofi Aventis; and PK-THPP: 10 μmol/L final concentration) in 50 μL dispensing volume. Mitochondrial membrane potential breakdown was assessed using the cationic dye JC-1 (Thermo Fisher Scientific). Cells were prepared as described earlier but were incubated with 15 μmol/L JC-1. The excitation wavelength was set to 515 nm and emission was detected at 535 nm and 595 nm. The Fenton reaction and superoxide formation were assessed using 2′,7′-dichlorofluorescin diacetate and MitoSOX (both Thermo Fisher Scientific), according to the manufacturer's recommendations. Assays for function of the mitochondrial electron transport chain were conducted 30 minutes after DSS exposure.

Immunofluorescence Staining

Immunohistochemistry was performed as described before.[22] The following antibodies were used: rabbit anti-mouse-Task1 (P0981, 1:250; Sigma Aldrich), rabbit anti-mouse-Task3 (P5247, 1:250; Sigma Aldrich), and rabbit anti-mouse–caspase 3 p17 (ab13847, 1:250; Abcam). A goat anti-rabbit IgG–Alexa Fluor 488-conjugate (A27034, 1:500; Thermo Fisher Scientific) was used as the secondary antibody. For visualizing cell nuclei within immunofluorescent stainings, sections were embedded in Fluoromount-G with 4',6-diamidino-2-phenylindole (Thermo Fisher Scientific) before microscopic analysis.

Statistical Analysis

Statistical analysis was conducted using IBM SPSS Statistics 28.0 (IBM), and graphs were created using PRISM 9.0.0 (GraphPad Software). Significance was evaluated using 2-way analysis of variance including the Bonferroni post hoc test for clinical data from DSS-induced colitis models. Column statistics were performed using the Mann–Whitney *U* test for comparison of 2 groups or the Kruskal–Wallis test including the Dunn post hoc test for comparison of multiple groups. A *P* value less than .05 was considered statistically significant.

References

1. Enyedi P, Czirjak G. Molecular background of leak K+ currents: two-pore domain potassium channels. Physiol Rev 2010;90:559–605.
2. Bittner S, Budde T, Wiendl H, Meuth SG. From the background to the spotlight: TASK channels in pathological conditions. Brain Pathol 2010;20:999–1009.
3. Meuth SG, Bittner S, Meuth P, Simon OJ, Budde T, Wiendl H. TWIK-related acid-sensitive K+ channel 1

(TASK1) and TASK3 critically influence T lymphocyte effector functions. J Biol Chem 2008;283:14559–14570.
4. Bittner S, Bauer MA, Ehling P, Bobak N, Breuer J, Herrmann AM, Golfels M, Wiendl H, Budde T, Meuth SG. The TASK1 channel inhibitor A293 shows efficacy in a mouse model of multiple sclerosis. Exp Neurol 2012; 238:149–155.
5. Saadati HR, Wittig M, Helbig I, Hasler R, Anderson CA, Mathew CG, Kupcinskas L, Parkes M, Karlsen TH, Rosenstiel P, Schreiber S, Franke A. Genome-wide rare copy number variation screening in ulcerative colitis identifies potential susceptibility loci. BMC Med Genet 2016;17:26.
6. Wilke BU, Lindner M, Greifenberg L, Albus A, Kronimus Y, Bunemann M, Leitner MG, Oliver D. Diacylglycerol mediates regulation of TASK potassium channels by Gq-coupled receptors. Nat Commun 2014;5:5540.
7. Bista P, Pawlowski M, Cerina M, Ehling P, Leist M, Meuth P, Aissaoui A, Borsotto M, Heurteaux C, Decher N, Pape HC, Oliver D, Meuth SG, Budde T. Differential phospholipase C-dependent modulation of TASK and TREK two-pore domain K+ channels in rat thalamocortical relay neurons. J Physiol 2015; 593:127–144.
8. Cahalan MD, Chandy KG. The functional network of ion channels in T lymphocytes. Immunol Rev 2009; 231:59–87.
9. Czirjak G, Enyedi P. Formation of functional heterodimers between the TASK-1 and TASK-3 two-pore domain potassium channel subunits. J Biol Chem 2002; 277:5426–5432.
10. Samak G, Chaudhry KK, Gangwar R, Narayanan D, Jaggar JH, Rao R. Calcium/Ask1/MKK7/JNK2/c-Src signalling cascade mediates disruption of intestinal epithelial tight junctions by dextran sulfate sodium. Biochem J 2015;465:503–515.
11. Chang JT. Pathophysiology of inflammatory bowel diseases. N Engl J Med 2020;383:2652–2664.
12. Torres J, Mehandru S, Colombel JF, Peyrin-Biroulet L. Crohn's disease. Lancet 2017;389:1741–1755.
13. Nowacki TM, Bruckner M, Eveslage M, Tepasse P, Pott F, Thoennissen NH, Hengst K, Ross M, Bettenworth D. The risk of colorectal cancer in patients with ulcerative colitis. Dig Dis Sci 2015;60:492–501.
14. Zeng C, Long X, Cotten JF, Forman SA, Solt K, Faingold CL, Feng HJ. Fluoxetine prevents respiratory arrest without enhancing ventilation in DBA/1 mice. Epilepsy Behav 2015;45:1–7.
15. Srisomboon Y, Zaidman NA, Maniak PJ, Deachapunya C, O'Grady SM. P2Y receptor regulation of K2P channels that facilitate K(+) secretion by human mammary epithelial cells. Am J Physiol Cell Physiol 2018;314:C627–C639.
16. Ozoren N, Kim K, Burns TF, Dicker DT, Moscioni AD, El-Deiry WS. The caspase 9 inhibitor Z-LEHD-FMK protects human liver cells while permitting death of cancer cells exposed to tumor necrosis factor-related apoptosis-inducing ligand. Cancer Res 2000; 60:6259–6265.
17. Sammels E, Parys JB, Missiaen L, De Smedt H, Bultynck G. Intracellular Ca2+ storage in health and disease: a dynamic equilibrium. Cell Calcium 2010;47:297–314.
18. Das I, Png CW, Oancea I, Hasnain SZ, Lourie R, Proctor M, Eri RD, Sheng Y, Crane DI, Florin TH, McGuckin MA. Glucocorticoids alleviate intestinal ER stress by enhancing protein folding and degradation of misfolded proteins. J Exp Med 2013;210:1201–1216.
19. Nagy D, Gonczi M, Dienes B, Szoor A, Fodor J, Nagy Z, Toth A, Fodor T, Bai P, Szucs G, Rusznak Z, Csernoch L. Silencing the KCNK9 potassium channel (TASK-3) gene disturbs mitochondrial function, causes mitochondrial depolarization, and induces apoptosis of human melanoma cells. Arch Dermatol Res 2014;306:885–902.
20. Chokshi RH, Larsen AT, Bhayana B, Cotten JF. Breathing stimulant compounds inhibit TASK-3 potassium channel function likely by binding at a common site in the channel pore. Mol Pharmacol 2015;88:926–934.
21. Wan Y, Yang L, Jiang S, Qian D, Duan J. Excessive apoptosis in ulcerative colitis: crosstalk between apoptosis, ROS, ER stress, and intestinal homeostasis. Inflamm Bowel Dis 2022;28:639–648.
22. Albrecht S, Korr S, Nowack L, Narayanan V, Starost L, Stortz F, Arauzo-Bravo MJ, Meuth SG, Kuhlmann T, Hundehege P. The K2P-channel TASK1 affects Oligodendroglial differentiation but not myelin restoration. Glia 2019;67:870–883.
23. Meuth SG, Herrmann AM, Ip CW, Kanyshkova T, Bittner S, Weishaupt A, Budde T, Wiendl H. The two-pore domain potassium channel TASK3 functionally impacts glioma cell death. J Neurooncol 2008;87:263–270.
24. Nakakura S, Matsui M, Sato A, Ishii M, Endo K, Muragishi S, Murase M, Kito H, Niguma H, Kurokawa N, Fujii M, Araki M, Araki K, Ohya S. Pathophysiological significance of the two-pore domain K(+) channel K2P5. 1 in splenic CD4(+)CD25(-) T cell subset from a chemically-induced murine inflammatory bowel disease model. Front Physiol 2015;6:299.
25. Feske S. CRAC channels and disease - from human CRAC channelopathies and animal models to novel drugs. Cell Calcium 2019;80:112–116.
26. Concepcion AR, Feske S. Regulation of epithelial ion transport in exocrine glands by store-operated Ca(2+) entry. Cell Calcium 2017;63:53–59.
27. Guo C, Sun L, Chen X, Zhang D. Oxidative stress, mitochondrial damage and neurodegenerative diseases. Neural Regen Res 2013;8:2003–2014.
28. Mancini NL, Goudie L, Xu W, Sabouny R, Rajeev S, Wang A, Esquerre N, Al Rajabi A, Jayme TS, van Tilburg Bernandes E, Nasser Y, Ferraz JGP, Shutt T, Shearer J, McKay DM. Perturbed mitochondrial dynamics is a novel feature of colitis that can be targeted to lessen disease. Cell Mol Gastroenterol Hepatol 2020;10:287–307.
29. Malhotra JD, Kaufman RJ. ER stress and its functional link to mitochondria: role in cell survival and death. Cold Spring Harb Perspect Biol 2011;3:a004424.
30. Wrzosek A, Augustynek B, Zochowska M, Szewczyk A. Mitochondrial potassium channels as druggable targets. Biomolecules 2020;10:1200.

31. Bachmann M, Li W, Edwards MJ, Ahmad SA, Patel S, Szabo I, Gulbins E. Voltage-gated potassium channels as regulators of cell death. Front Cell Dev Biol 2020;8:611853.
32. Johnstone LS, Graham SJ, Dziadek MA. STIM proteins: integrators of signalling pathways in development, differentiation and disease. J Cell Mol Med 2010;14:1890–1903.
33. Rusznak Z, Bakondi G, Kosztka L, Pocsai K, Dienes B, Fodor J, Telek A, Gonczi M, Szucs G, Csernoch L. Mitochondrial expression of the two-pore domain TASK-3 channels in malignantly transformed and non-malignant human cells. Virchows Arch 2008;452:415–426.
34. Kalkavan H, Green DR. MOMP, cell suicide as a BCL-2 family business. Cell Death Differ 2018;25:46–55.
35. Huai J, Vogtle FN, Jockel L, Li Y, Kiefer T, Ricci JE, Borner C. TNFalpha-induced lysosomal membrane permeability is downstream of MOMP and triggered by caspase-mediated NDUFS1 cleavage and ROS formation. J Cell Sci 2013;126:4015–4025.
36. Cotten JF. TASK-1 (KCNK3) and TASK-3 (KCNK9) tandem pore potassium channel antagonists stimulate breathing in isoflurane-anesthetized rats. Anesth Analg 2013;116:810–816.
37. Babickova J, Tothova L, Lengyelova E, Bartonova A, Hodosy J, Gardlik R, Celec P. Sex differences in experimentally induced colitis in mice: a role for estrogens. Inflammation 2015;38:1996–2006.
38. Siegmund B, Lehr HA, Fantuzzi G, Dinarello CA. IL-1 beta -converting enzyme (caspase-1) in intestinal inflammation. Proc Natl Acad Sci U S A 2001;98:13249–13254.
39. Kwon SH, Florens L, Swanson SK, Washburn MP, Abmayr SM, Workman JL. Heterochromatin protein 1 (HP1) connects the FACT histone chaperone complex to the phosphorylated CTD of RNA polymerase II. Genes Dev 2010;24:2133–2145.

Received May 3, 2021. Accepted August 10, 2022.

Correspondence
Address correspondence to: Sven G. Meuth, MD, PhD, Department of Neurology, University Hospital Duesseldorf, Heinrich-Heine-University Duesseldorf, Moorenstraße 5, D-40225 Duesseldorf, Germany. e-mail: meuth@uni-duesseldorf.de.

Acknowledgements
The authors would like to thank Iska Loesmann and Jeannette Budde for their expert technical support.

CRediT Authorship Contributions

Steffen Pfeuffer, MD (Data curation: Lead; Formal analysis: Lead; Writing – original draft: Lead)

Thomas Muentefering, MSc (Formal analysis: Equal; Methodology: Equal; Writing – review & editing: Supporting)

Leoni Rolfes, MD (Data curation: Supporting; Writing – review & editing: Supporting)

Frederike Anne Straeten, MD (Data curation: Supporting; Writing – review & editing: Supporting)

Susann Eichler, PhD (Data curation: Supporting; Formal analysis: Supporting; Writing – review & editing: Supporting)

Joel Gruchot, MSc (Data curation: Supporting; Formal analysis: Supporting)

Vera Dobelmann, MSc (Data curation: Supporting)

Tim Prozorovski, PhD (Data curation: Supporting)

Boris Görg, PhD (Data curation: Supporting; Formal analysis: Supporting)

Mihael Vucur, PhD (Data curation: Supporting; Formal analysis: Supporting)

Carsten Berndt, PhD (Data curation: Supporting; Formal analysis: Supporting; Writing – review & editing: Supporting)

Patrick Küry, PhD (Writing – review & editing: Supporting)

Tobias Ruck, MD (Formal analysis: Supporting; Writing – review & editing: Supporting)

Stefan Bittner, MD (Conceptualization: Supporting; Writing – review & editing: Supporting)

Dominik Bettenworth, MD (Methodology: Supporting; Writing – review & editing: Supporting)

Thomas Budde, PhD (Writing – review & editing: Supporting)

Tom Luedde, MD, PhD (Methodology: Supporting; Writing – review & editing: Supporting)

Sven G Meuth, MD, PhD (Conceptualization: Lead; Project administration: Lead; Writing – review & editing: Equal)

Conflicts of interest
The authors disclose no conflicts.

Funding
This work was supported by the Innovative Medical Research fund of the University of Muenster I-PF211701 (S.P.).